American Mineralogist, Volume 68, pages 477–493, 1983

Pyroxene thermometry[1]

DONALD H. LINDSLEY

Department of Earth and Space Sciences
State University of New York, Stony Brook, New York, 11794

Abstract

Experimentally determined Ca–Mg–Fe pyroxene phase relations at 800–1200°C and from less than one atmosphere up to 15 kbar are combined with calculated phase equilibria for the diopside–enstatite and hedenbergite–ferrosilite joins to produce a graphical two-pyroxene thermometer applicable to a wide variety of rocks from the earth, moon, and meteorites. Samples with appreciable contents of "others" components require special projection onto the Di–En–Hd–Fs pyroxene quadrilateral; Wo, En, and Fs components as normally calculated will *not* yield correct temperatures. The projection approximates the activities of those components in natural pyroxenes but is largely empirical, and may not be appropriate for large contents of nonquadrilateral components. Therefore, the thermometer should be used only for pyroxenes having Wo + En + Fs ≥ 90%. The effects of pressure are ≤8°C/kbar; graphs are presented for relations at one atmosphere and at 5, 10, and 15 kbar, along with approximate formulas for interpolating between these pressures. The occurrence of granule exsolution—the coalescence of exsolved pyroxene, with possible migration to grain boundaries—can complicate the use of the thermometer for slowly cooled rocks. The primary pyroxene compositions must be reconstructed from textural evidence before correct igneous or peak-metamorphic temperatures can be inferred.

The experimental data and inferred temperatures for three-pyroxene assemblages permit calibration of an improved pigeonite thermometer.

Introduction

Petrologists have long recognized the potential of coexisting high-Ca and low-Ca pyroxenes to yield thermometric information for a wide variety of rocks (Table 1; Fig. 1). In particular, the Ca content of high-Ca pyroxene (augite) decreases with increasing temperature, while that of the low-Ca phase (orthopyroxene or pigeonite) increases. Although there may also be thermometric information in the distribution of Mg and Fe between the high-Ca and low-Ca pyroxenes (see, for example, Kretz, 1982) this paper is concerned only with Ca partitioning, in part because there are more experimental data available for the Ca contents than for the Mg–Fe distributions of coexisting pyroxenes. The two-pyroxene thermometer presented here yields temperatures of formation for many rocks from the moon, earth, and meteorites.

Previous two-pyroxene thermometers

Most two-pyroxene thermometers have been designed for pyroxene pairs whose compositions plot near the Di–En–Hd–Fs quadrilateral (Fig. 1)—that is, Wo + En + Fs usually total 90% or more. With but few exceptions, the thermometers involve at least two steps: projection onto the quadrilateral, followed by application of relations in the quadrilateral (or a part thereof) to obtain temperatures. A successful thermometer must accomplish both these steps adequately. This paper will show that only the two-pyroxene thermometers of Kretz (1982; Ca reaction), Lindsley and Andersen (1983), and Ross and Huebner (1975) are successful over a wide range of temperatures and pyroxene compositions, although the Ross–Huebner thermometer tends to underestimate temperatures for some igneous pyroxenes by approximately 50°C.

The most frequently used thermometers project the quadrilateral compositions to the Di–En (Fe-free) join and employ either a phase diagram or solution model for that join to yield temperatures. This approach was pioneered by Boyd (*e.g.*, Davis and Boyd, 1966; Boyd, 1969; Boyd, 1973), who used simple projections of Fe-poor pyroxenes onto the Di–En phase diagram. Following Boyd, almost all two-pyroxene thermometers have treated the effects of pressure as negligible. A major step forward was made by Wood and Banno (1973), who developed a simple solution model for the Di–En join and presented an analytical expression for temperature based on the estimated enthalpy of the reaction orthoenstatite = clinoenstatite (OEn = CEn). Wells (1977) revised this thermometer on

[1]Presidential Address, Mineralogical Society of America. Delivered at the 63rd Annual Meeting of the Society, October 19, 1982.

0003–004X/83/0506–0477$02.00

Table 1. Pyroxenes as geothermometers

A. One-Pyroxene Thermometers:

1. Ca content of Augite or Orthopyroxene - minimum T
2. Pigeonite - minimum T
3. Protopyroxene - minimum T

B. Two-Pyroxene Thermometers:

1. Ca contents of coexisting augite-orthopyroxene; augite-pigeonite; pigeonite-orthopyroxene pairs
2. Orientation of two-pyroxene tie lines: e.g., distribution of Mg and Fe between augite and orthopyroxene

C. Three-Pyroxene Thermometer:

1. Augite + pigeonite + orthopyroxene can coexist at only one T for a given pressure and Fe/(Fe + Mg); affected by "others" components

D. Related thermometer:

1. Hedenbergite-ferrobustamite relations (Skaergaard)

the basis of newer, reversed experimental data on the Di–En join. Both of these thermometers continue in wide use, although their assumptions of ideal mixing in clinopyroxene and a large reaction enthalpy for OEn = CEn are seriously in error (Holland *et al.*, 1979; Lindsley *et al.*, 1981; Davidson *et al.*, 1982). At high temperatures, the errors introduced by these assumptions tend to be self-cancelling; for metamorphic pyroxenes the temperatures are 100°C or more too high. In view of the recent improvements in solution models of the Di–En join, use of these thermometers is an anachronism that should be avoided. Saxena and Nehru (1975), Saxena (1976), Mercier (1976), and Kretz (1982) also presented thermometers that involve projection to the Di–En join. Saxena and Nehru made the important point that both the clinopyroxene and orthopyroxene series must be treated as distinct, nonideal solutions. Mercier emphasized that each pyroxene of a pyroxene pair contains thermometric information, and he also advocated inclusion of the effects of pressure. Kretz' thermometer is the most successful, probably because his projection to the Di–En join involved a careful evaluation of both igneous and metamorphic pyroxenes.

Other workers have attempted to use phase relations within the quadrilateral, natural occurrences, or a combination of both to determine temperatures. The three-pyroxene (augite + pigeonite + orthopyroxene) thermometer of Ishii (1975) was based mainly on observed temperatures of two erupting lavas. The pyroxenes of these lavas are rather similar in composition, so the effective calibration is limited to X [= Fe/(Fe+Mg)] values near 0.25 to 0.35. Ross and Huebner (1979) and Podpora and Lindsley (1979) also presented thermometers based on the minimum stability of pigeonite. But each of these thermometers is appropriate over only a limited range of X values (Lindsley and Andersen, 1983); the Ishii and Ross–Huebner curves seem to be better for natural samples having X from 0.3 to 0.5, whereas the Podpora–Lindsley curve is preferred for Fe-rich samples. Ishii (1981) attempted to extend his thermometer to two-pyroxene assemblages by adopting the Wood–Banno formalism for augite–orthopyroxene as well as augite–pigeonite equilibria, but this approach also leads to unacceptably high enthalpies for the OEn–CEn reaction. Furthermore, his assumption of a large reaction enthalpy for the augite + pigeonite pair is inappropriate because these clinopyroxenes appear to obey the same equation of state at high temperatures (Lindsley *et al.*, 1981). Accordingly I recommend that this thermometer not be used.

The Ross and Huebner graphical thermometer (1975) was based on unreversed experimental data at high temperatures (mainly above 1000°C) and on petrologic intuition at lower temperatures. Topologically their diagram is closely similar to the one-atmosphere diagram presented here. The two thermometers give virtually identical temperatures for metamorphic pyroxenes. Kretz (1982) derived two two-pyroxene thermometers, one based on the distribution of Mg and Fe and the other on the partitioning of Ca between augite and low-Ca pyroxene. Kretz' Mg–Fe thermometer greatly overestimates temperatures for some experimentally equilibrated pyroxenes (Lindsley and Andersen, 1983). In contrast, his Ca thermometer gives results that are closely similar to those of the thermometer presented here and by Lindsley and Andersen (1983).

Attempts to use phase-equilibrium data for quadrilateral pyroxenes (Lindsley *et al.* 1974; Lindsley, 1980) to

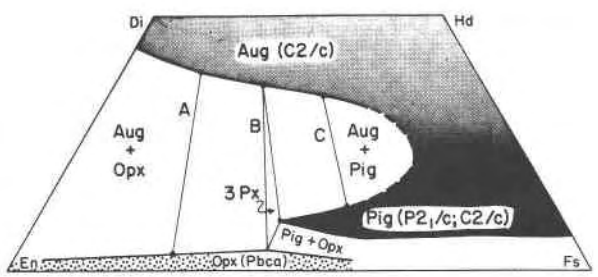

Fig. 1. Schematic representation of pyroxene relations in the Di–En–Hd–Fs quadrilateral (at some arbitrary pressure and temperature), showing the two- and three-pyroxene assemblages that can be used for geothermometry. A, augite + orthopyroxene; B, augite + orthopyroxene + pigeonite; C, augite + pigeonite. The $CaSiO_3$ (Wo) content of each pyroxene yields an independent estimate of temperature. The augite + pigeonite field (C) ends at a consolute point, to the right of which there is a continuous clinopyroxene field because pigeonite at high temperature has the same space group as augite. At low pressures this continuous clinopyroxene field is metastable with respect to melting and/or to the assemblage augite + olivine + silica. Depending on pressure and temperature, other portions of the diagram may be metastable with respect to protopyroxene, pyroxenoid, or olivine + liquid. Relations near Fs are omitted.

extract thermometric information from complex natural pyroxenes have not been very successful, at least in part because the effects of nonquadrilateral components in the latter were not accounted for. For example, Figure 2 shows the trend for Mg-rich Skaergaard augites (Brown, 1957) superimposed on the 900°C, 1 kbar, augite solvus (stippled area) of Turnock and Lindsley (1981). Not only are the apparent temperatures unreasonably low, but also it appears that temperature increased with increasing Fe/(Fe+Mg)! Possible causes of these discrepancies are: (1) natural pyroxenes require a special projection onto the quadrilateral to provide a realistic estimate of the activities of Wo, En, and Fs; and (2) the Mg-rich Skaergaard augites have reequilibrated to subsolidus temperatures (Lindsley and Andersen, 1983). A successful thermometer must be based both on experimental data of high quality and on an understanding of the effects of the nonquadrilateral components. Lindsley and Andersen (1983) derived a (mainly empirical) projection scheme that approximates the activities of Wo, En, and Fs in natural pyroxenes, thereby permitting the use of quadrilateral phase relations for thermometry. The present paper is an expansion of their work.

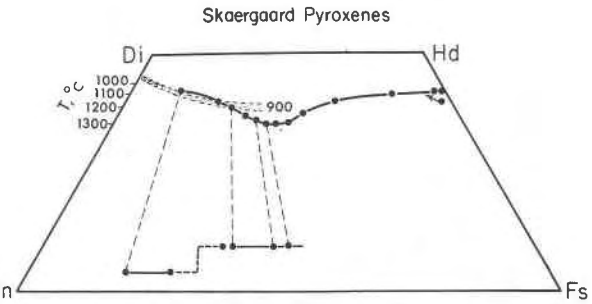

Fig. 2. The Mg-rich augite trend from the Skaergaard intrusion (Brown, 1957; dots and heavy line), superimposed on the 900°C, 1 kbar augite solvus (stippled band) of Turnock and Lindsley (1981). Both the apparent temperatures of the augites and the apparent increase in temperature with increasing Fe are contrary to petrologic expectation. Temperatures on the Di–En join are calculated from Lindsley *et al.*, 1981.

The new two-pyroxene thermometer

The approach to the present graphical two-pyroxene thermometer is twofold: (1) Determination of phase equilibria for pure Ca–Mg–Fe pyroxenes over a wide range of pressures and temperatures, since these relations contain the basic thermometric information. (2) Assessment of the effects of nonquadrilateral components on the activities of the Wo, En, and Fs components. The first part is virtually complete; the second is really just beginning. Additional data on the effects of the nonquadrilateral components will surely require modifications of the projection scheme, but the graphs themselves are expected to need little if any change. Thermodynamic solution models now being developed for quadrilateral pyroxenes will ultimately permit direct calculation of temperatures from compositions of coexisting pyroxenes, but the graphical thermometers should be useful in the meantime.

Experimental calibration

Details of the low-pressure (<one atmosphere to 2 kbar) experiments are given by Turnock and Lindsley (1981) and by Lindsley and Andersen (1983). This paper presents data for experiments at 15 kbar.

Starting materials

Starting materials for the phase-equilibrium experiments were prepared following the methods of Turnock *et al.* (1973), and were characterized by means of X-ray diffraction, electron probe microanalysis, and optical examination. Approximately one-half of the phases were synthesized by Turnock at one atmosphere in a gas-mixing furnace; most of the others were synthesized hydrothermally at 15–20 kbar, 950–1000°C. Phases with intermediate Ca contents (20–30 mole% Wo) served as starting materials for exsolving experiments; trace amounts (≪1%) of orthopyroxene were added to some to provide seeds for the growth of orthopyroxene. Finely ground mechanical mixtures of high-Ca and low-Ca pyroxenes served as starting materials for dissolving experiments. Details of each starting material are given in Table 2.

Table 2. Starting materials

Index	Bulk Wo	Comp. X	P H A S E (S) Aug (Cpx)* Wo	X	Low-Ca** Wo	X
A	30	0.10	Cpx (zoned in Wo)			
B	30	0.10	50	0.20	0	0.025(O)
C	30	0.10	46.2	0.0	0	0.20(O)
D	20	0.20	Cpx (zoned in Wo: 15-27)			
E	25	0.20	50	0.20	0	0.20(O)
F	25	0.20	50	0.0	0	0.30(O)
G	30	0.30	Cpx			
H	30	0.30	50	0.30	0	0.30(O)
I	28.5	0.30	50	0.0	0	0.50(O)
J	30	0.30	50	0.0	4	0.50(P)
K	25	0.40	40	0.50	0	0.30(O)
L	25	0.40	40	0.30	0	0.50(O)
M	30	0.50	Cpx			
N	30	0.50	50	0.50	4	0.50(P)
O	25	0.50	50	0.30	0	0.60(O)
P	20	0.60	Cpx			
R	25	0.60	Cpx			
S	30	0.60	Cpx			
T	20	0.60	40	0.60	0	0.60(O)
U	25	0.60	40	0.60	10	0.60(P)
V	20	0.60	40	0.30	5	0.75(O)
W	20	0.75	Cpx			
X	25	0.75	Cpx			
Y	20	0.75	45	0.75	0	0.75(O)
Z	25	0.75	50	0.75	0	0.75(O)
AA	25	0.75	45	0.75	10	0.75(P)
BB	25	0.75	40	0.60	10	0.85(P)
CC	25	0.75	50	0.60	0	0.80(O)
DD	25	0.85	Cpx			
EE	25	0.85	45	0.85	0	0.85(O)
FF	25	0.85	45	0.75	0	0.92(O)
GG	25	0.85	35	0.85	15	0.85(P)
HH	25	0.85	35	0.75	15	0.92(P)

Wo is mole percent $CaSiO_3$. X = Fe/(Fe + Mg).
*Cpx means single phase (zoned in some cases)
**Low-Ca phase is orthopyroxene (O) or clinopyroxene (P).

Experiments at 15 kbar

The experiments at 15 kbar expand the range of those reported by Lindsley *et al.* (1974). Each experiment contained the desired pyroxene (or mechanical mixture of pyroxenes) sealed in a silver capsule with approximately 10 wt.% water, 3–5 wt.% excess SiO_2 to saturate the vapor phase, and a trace (<1 wt.%) of oxalic acid to inhibit oxidation. Most of the points are bracketed by triplets of experiments: (1) exsolving experiments from single-phase clinopyroxenes of intermediate Wo content, (2) dissolving experiments with mechanical mixtures of high-Ca and low-Ca pyroxenes having the same X values, and (3) dissolving experiments with mechanical mixtures of Ca-rich, Mg-rich augites and Ca-poor, Mg-poor orthopyroxenes (or pigeonites). Such triplets bracket the distribution of Mg and Fe as well as of Ca between the coexisting phases. The furnace assemblies and experimental procedures are similar to those described by Lindsley (1981). The redox conditions of the experiments were sufficiently low to prevent formation of magnetite; however, Mössbauer measurements to detect possible ferric iron in the run products have not been made.

Analytical techniques

The products of each experiment were examined under the petrographic microscope and by powder X-ray diffraction. Wo contents of clinopyroxenes were estimated from X-ray data using determinative curves (calculated from the data of Turnock *et al.* 1973) for the (220), (22$\bar{1}$), (310), (31$\bar{1}$), (002), (211), and (311) reflections. If the X-ray results indicated that pairs or triplets of exsolving and dissolving experiments had come substantially to equilibrium (as shown by closely similar patterns for the runs), the samples were mounted in epoxy and polished for electron microprobe analysis. The microprobe used was the Stony Brook ARL-EMX automated system, with the Bence–Albee and Albee–Ray correction schemes. Operating conditions were 15 kV, beam integration, beam current of 0.17 to 0.18 microamps, specimen current of 0.015 microamps on brass, and minimum spot size (approx. one square micron). Standards were Y6 diopside and a synthetic orthopyroxene $Wo_4En_{24}Fs_{72}$. Microprobe analysis of fine-grained and often zoned run products can lead in some cases to ambiguous results (see, for example, discussions by Lindsley and Dixon, 1976, and Turnock and Lindsley, 1981). The compositions listed in the data table and plotted in the figures represent interpretations of data that involved varying amounts of compositional zoning and grain overlap. Usually, however, the combination of microprobe and X-ray diffraction data permits a unique interpretation of the results. The results reported here for some 15 kbar experiments show somewhat different Wo contents from those illustrated by Lindsley (1980), mainly because greater weight has been assigned to the Ca contents indicated by the X-ray diffraction data. Figure 3 illustrates the logic in this decision. Microprobe analysis of the product augites yields a range of apparent Wo contents. In contrast, the X-ray diffraction peaks are all sharp and indicate that the augite is $Wo_{34\pm1}$, with X in the range 0.52–0.62. Accordingly, the run symbol (an arrowhead pointing away from the starting augite) for augite is plotted at Wo_{34}, $X = 0.57$, where the X-ray and probe plots intersect. I interpret the more calcic probe points as representing incomplete reaction, and the less calcic ones as resulting from grain overlap with pigeonite; note that the latter fall on a mixing line between Wo_{34} and the product pigeonite. Figure 12c (mislabeled 12a) of Lindsley (1980) had accepted the cluster of probe analyses at Wo_{28-29} as representing the composition of the product augite of this experiment, and accordingly the augite solvus was drawn at a lower Wo content than shown in the present paper. The experimental results at 15 kbar are summarized in Table 3.

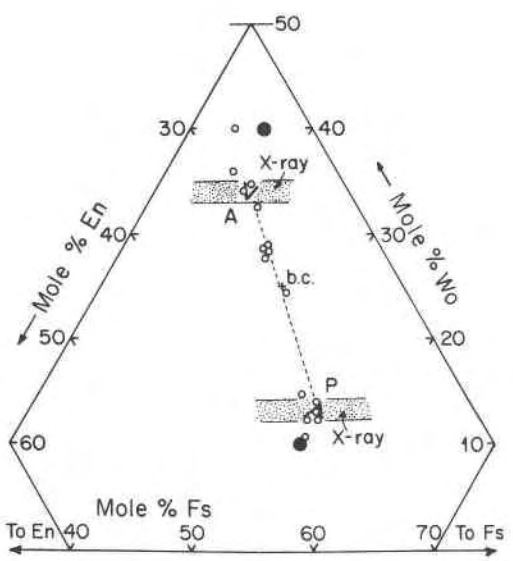

Fig. 3. A portion of the pyroxene quadrilateral, showing microprobe analyses, and Wo contents from X-ray determinative curves, of the products of a dissolving experiment at 990°C, 15 kbar. Filled circles show the starting phases; + b.c. shows the bulk composition of the experiment. Small open circles are microprobe analyses of individual product crystals. Wo contents determined by both methods are in close agreement for the pigeonites (P). However, the augites (A) show an apparent spread in Wo content that is considered to reflect both incomplete reaction and grain overlap with pigeonites. The data symbols (arrowheads) are drawn so as to be compatible with both the microprobe and the X-ray data.

Construction of the two-pyroxene thermometer

The two-pyroxene thermometer for the quadrilateral has been constructed on the basis of (1) phase equilibria at and near one atmosphere, including calculated phase diagrams for the Di–En and Hd–Fs joins; (2) estimates of the temperature of the consolute point for augite–pigeonite as a function of X; (3) the minimum stability of pigeonite, also as a function of X; and (4) the effects of pressure.

Table 3. Hydrothermal experiments at 15 kbar

Start. Mtl.	T, °C	Duration d	h	RUN X-ray Aug Wo	Low-Ca** Wo	PRODUCTS* Microprobe Aug Wo	X	Opx Wo	X	Pig Wo	X
A	990	2	22	42	3(O)	44	.08	2.5	.125		
B	990	2	17	41	3(O)	43	.10	2	.13		
C	990	2	23	42	3(O)	43	.09	2	.12		
D	990	3	5	39	4(O)	41	.17	3.5	.215		
E	990	0	17	38	4(O)	39	.18	3	.22		
F	990	3	5	39	4(O)	40	.19	3.5	.23		
G	990	2	22	37	4(O)	39	.285	3	.34		
H	990	2	6	37	Opx	39	.28	3	.335		
I	990	3	20	38	3(O)	38.5	.29	3.5	.35		
J	990	2	6	37	Opx	38.5	.30	4.5	.36		
K	990	2	18	37	Opx	37	.37	3.5	.43		
L	990	3	0	37	Opx	38	.37	3.5	.42		
M	990	3	10	35	Opx	34	.48	4.5	.53		
N	990	3	22	35	Opx	34	.50	5	.535		
O	990	3	10	34	Opx	33.5	.49	4.5	.53		
R	990	2	7	32	14(P); Opx	30	.57	4.5	.61	-	-
T	980	3	8	35	4(O); Pig	34.5	.55	4.5	.605	-	-
U	990	3	2	34	14(P)	34	.57			13	.615
V	980	3	8	35	5(O)	35	.535	5	.62		
D	910	8	7	42	3(O)	43	.16	2.5	.215		
E	910	3	15	41	3(O)	43	.17	2	.22		
P	910	6	19	36	4(O)	36	.565	4.5	.62		
T	910	7	4	37	3(O)	37	.57	4	.63		
V	910	6	19	37	4(O)	37	.555	4	.63		
W	910	6	18	33	4(O)	31	.73	4.5	.765		
X	915	15	0	32	14(P)	33	.735			13	.79
Y	900	14	13	36	4(O)	33	.725	4	.76		
AA	925	6	12	33	14(P)	32	.73			15	.755
BB	925	11	17	32	13(P)	32	.72	4.5	.765	12	.78
DD	910	6	15	30	15(P)	29	.83			16	.855
GG	915	5	21	33	15(P)	31	.83			18	.855
HH	915	5	21	31	15(P)	29	.83			19	.865
A	810	16	8	43	2(O); Amph	45	.085	1.5	.14		
B	810	16	8	44	2(O); Amph	44.5	.10	1	.09		
C	810	16	16	43	2(O); Amph	44	.09	1.2	.14		
D	810	25	19	42	2(O)	42	.16	2	.235		
E	810	14	20	42	3(O)	44	.17	2.5	.24		
F	810	13	15	41	Opx	44	.17	2	.25		
G	815	14	0	40	Opx; Amph	39	.30	3	.395		
H	815	17	3	40	4(O)	42	.27	2.5	.36		
I	810	13	15	41	3(O)	41	.26	2	.395		
G	810	16	22	42	Opx	42	.28	-	-		
K	810	18	1	40	4(O)	40	.35	2.5	.44		
L	810	18	1	40	4(O)	40	.355	2.5	.43		
M	815	13	21	38	3(O)	39	.47	3	.56		
N	815	14	0	39	3(O)	40	.465	3.5	.56		
O	815	14	0	40	3(O)	40	.44	3	.55		
P	815	14	7	38	4(O)	39	.55	4	.625		
S	815	13	21	38	4(O)	39	.55	3	.655		
T	815	12	0	38	3(O)	40	.54	3.5	.62		
V	815	12	0	37	3(O)	38	.55	4	.635		
X	815	14	3	40	3(O)	35.5	.72	3.5	.785		
Z	810	19	17	39	3(O)	39	.72	4	.77		
AA	810	11	16	37	3(O)	35	.73	4	.79		
CC	810	19	17	37	3(O)	39	.72	4	.77		
DD	810	14	23	35	4(O)	35	.835	4	.865		
EE	810	14	23	37	4(O)	34.5	.835	4.5	.86		
FF	810	14	15	35	4(O)	34.5	.835	4	.87		

*Compositions are ±1 mole percent. **(O) means orthopyroxene, (P) means pigeonite analysis. Opx, Pig, Amph mean orthopyroxene, pigeonite, or amphibole detected optically or by x-rays. -, present but not analysed.

1. Isothermal phase relations at or near one atmosphere. Experimental data on pyroxene equilibria at 800, 900, 1000, 1100, and 1200°C at low pressures, together with calculated phase diagrams for the Di–En and Hd–Fs joins (Figs. 4 and 5), yield a set of mutually consistent isothermal phase diagrams for Ca–Mg–Fe pyroxenes at or near one atmosphere (Figs. 6a–e). The requirement for mutual consistency has resulted in some revisions in the phase boundaries reported by Turnock and Lindsley (1981) at 900° and 1000°C, but for the most part the new boundaries remain consistent with their data (Figs. 6b and 6c).

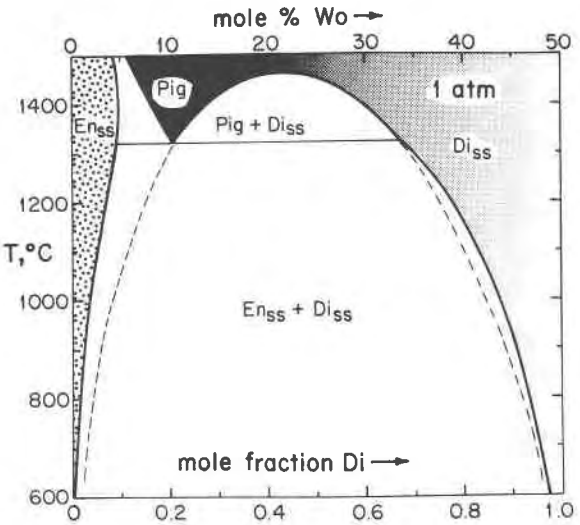

Fig. 4. Phase relations for the join Di–En at one atmosphere, Calculated from the solution model of Lindsley *et al.* (1981). At high temperatures, some of the relations shown may be metastable with respect to liquid (with or without olivine) or to protopyroxene or both.

2. Consolute line for the augite–pigeonite miscibility gap. The trace of the consolute point (Fig. 7) was constructed using the Fe-free and Mg-free endpoints (Figs. 4 and 5) as well as the data from Figures 6d and 6e, in which the two clinopyroxene fields so nearly merge that the consolute points can be estimated with considerable confidence. At one atmosphere, this consolute line is mainly or wholly metastable with respect to melting or other phase changes, but it still serves as a useful guide

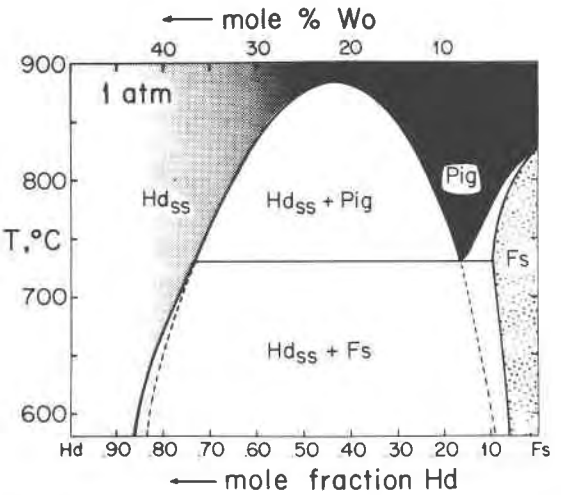

Fig. 5. Phase relations for the join Hd–Fs at one atmosphere, calculated from the solution model of Lindsley (1981). All the pyroxene relations shown are metastable with respect to olivine + silica + hedenbergite or ferrobustamite (see Lindsley and Munoz, 1969); the metastable relations are nevertheless very useful, as they provide important constraints on pyroxene relations within the quadrilateral.

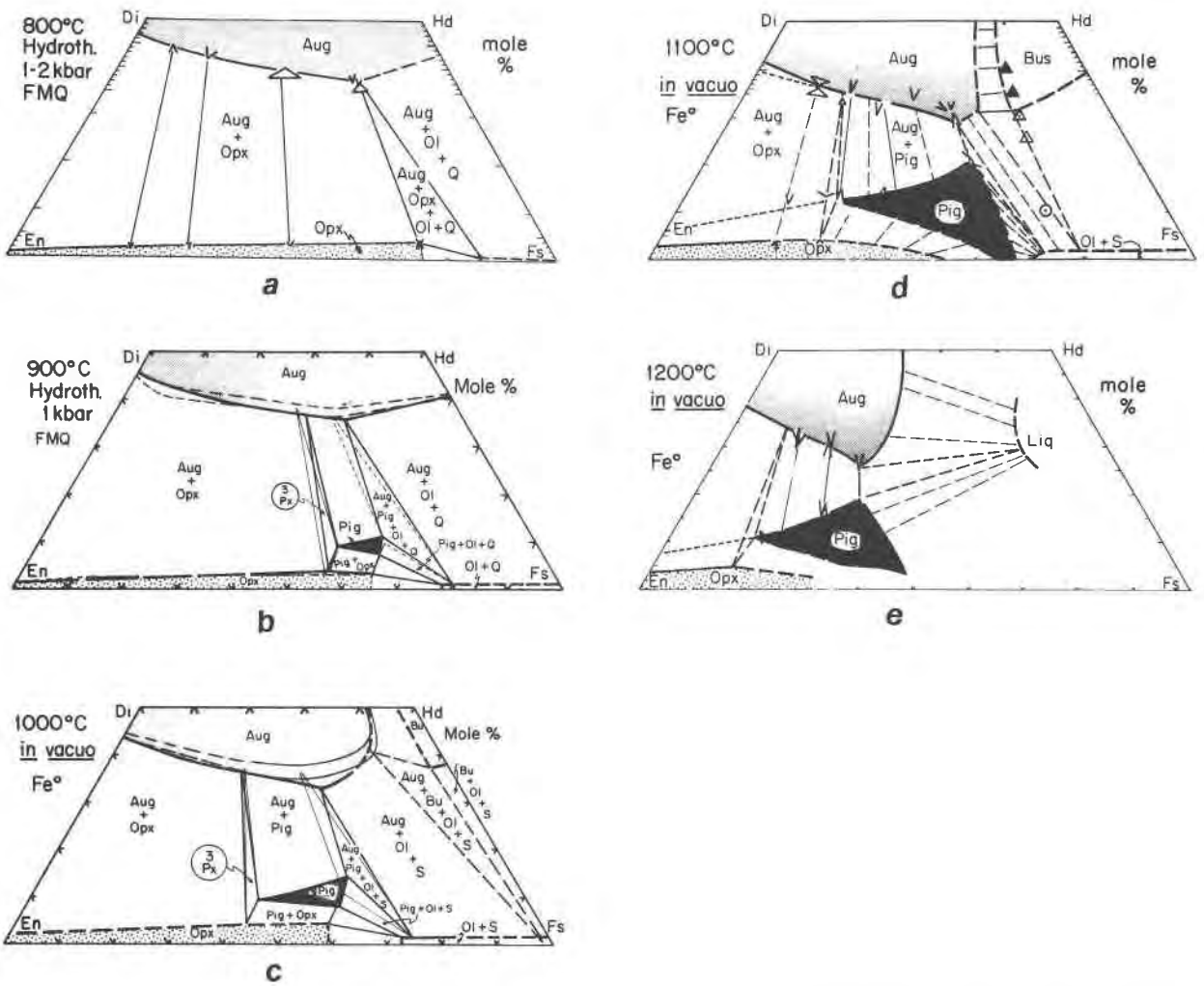

Fig. 6. Ca–Mg–Fe pyroxene phase relations at and near one atmosphere. Data symbols are arrowheads pointing the directions from which equilibrium was approached: V symbols are based on microprobe analyses, sometimes augmented by X-ray diffraction data (see Fig. 3). Open triangles give Wo contents based on X-ray diffraction only. In this and the following diagrams, the phase boundaries shown are constrained to be consistent with experiments at other temperatures as well as with the data points shown. Boundaries dashed where approximately located. Q = quartz; S means a silica polymorph, probably tridymite but possibly cristobalite. a. 800°C and 1 to 2 kbar. b. 900°C and 1 kbar; light lines show the boundaries of Turnock and Lindsley (1981), heavy lines the revised boundaries drawn to be mutually consistent with isotherms at lower and higher temperatures. c. 1000°C and $P <$ one atmosphere; line weights as in Figure 6b. d. 1100°C and $P <$ one atmosphere. Pyroxene symbols as in Figure 6a. Other symbols are: filled triangle, ferrobustamite; triangle with dot, ferrobustamite + olivine + silica; circle, augite + olivine + silica. e. Pyroxene relations at 1200°C and $P <$ one atmosphere. Symbols as in Figures 6a and 6d; Liq is liquid. Assemblages with olivine (Ol) and either Q or S constitute the "forbidden zone" within which pyroxenes are not stable at low pressures.

for constructing the stable portions of the two-clinopyroxene field. Both the binary solution models and experimental data at 15 kbar suggest that the consolute line is virtually unaffected by pressure.

3. Minimum stability of pigeonite. The plot for the minimum stability of pigeonite in Figure 8 is adapted from Podpora and Lindsley (1979) and Lindsley and Andersen (1983), with the effects of pressure added from Lindsley *et al.* (1981), Lindsley (1981), and the present results. It is emphasized that Figure 8 applies to the stability of pigeonite in the pure Ca–Mg–Fe system. The results of Ishii (1975) and of Ross and Huebner (1979) are probably more germane to Mg-rich natural pyroxenes, because these tend to contain appreciable amounts of non-quadrilateral components, which, being more abundant in augite and orthopyroxene, stabilize that assemblage relative to pigeonite. As a result, for fixed X the minimum temperature for pigeonite is raised. For a fixed temperature, the three-pyroxene triangles are displaced towards slightly high X-values. For consistency, the graphical thermome-

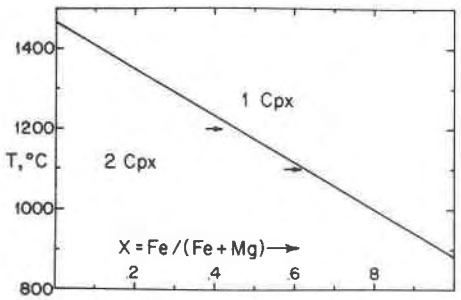

Fig. 7. Variation with X ($=Fe^{2+}/(Fe^{2+}+Mg)$) of the consolute temperature for augite + pigeonite. The arrows indicate minimum X values for the consolute temperatures at 1100° and 1200°C as estimated from Figures 6d and 6e.

ter is drawn according to the results for the pure Ca–Mg–Fe system; however, readers should be aware that the 1200° and 1100°C three-pyroxene triangles as drawn may need to be shifted a few mole percent to the right (and the orthopyroxene and augite solvi extrapolated accordingly) for applications of the thermometer to Mg-rich natural pyroxenes. The need for this shift will be illustrated by some of the applications to natural pyroxenes presented in a later section of this paper, along with a best estimate of the minimum stability of natural pigeonites.

4. Effects of pressure. Increasing pressure has three main effects on pyroxene equilibria: (1) the augite–orthopyroxene field widens at a given temperature; (2) the three-pyroxene triangles for each temperature become more Fe-rich; and (3) the "forbidden zone" becomes smaller, disappearing at around 11.5 kbar. The pressure effect on augite–orthopyroxene equilibria can be approximated by means of a simple interpolation between the Di–En and Hd–Fs joins, which leads to the estimated pressure corrections for the orthopyroxene and augite isotherms:

$$\text{augite: } T_P = T + (P - P^\circ)[1.63 - 2.104X + T(0.0027 + 0.0013X)]$$

$$\text{orthopyroxene: } T_P = T + (P - P^\circ)[0.33 - 0.98X + T(0.002 + 0.0075X)]$$

where T_P is the corrected temperature for pressure P (in kbar) and T is the apparent temperature indicated by the thermometer for pressure P°. For example, at an apparent T of 1000°C and $X = 0.50$, the temperature for augite increases by 3.9°C/kbar and that for orthopyroxene by 5.6°C/kbar. However, the pressure correction must vanish in the vicinity of three-pyroxene (augite + pigeonite + orthopyroxene) assemblages, because augite–pigeonite equilibria are nearly independent of pressure; excess volumes of the clinopyroxenes are very small (Turnock *et al.*, 1973; Lindsley *et al.*, 1981; Lindsley, 1981).

Superimposed, the isothermal diagrams (Figs. 6a–e) constitute a graphical two-pyroxene thermometer for low pressures (Fig. 9a). Isotherms below 800°C and above 1200°C are extrapolations from the Di–En and Hd–Fs joins, drawn to be consistent with the experimentally determined isotherms. The diagram omits most pigeonite–orthopyroxene relations (which are poorly constrained), melting, and the stability fields for protopyroxene and ferrobustamite. Within the "forbidden zone" at high X values, the diagram shows the metastable pyroxene relations within that zone (rather than the stable assemblages olivine + silica + augite or ferrobustamite) so as to facilitate the interpretation of pyroxenes that may form or persist in this region.

The effects of pressure can then be used to extrapolate Figure 9a to higher pressures. Graphical thermometers for pressures of 5, 10, and 15 kbar (Figs. 9b–d) have been constructed by applying the pressure dependence of pyroxene equilibria in the Di–En and Hd–Fs binaries as well as the pressure effect on the minimum stability of pigeonite (Fig. 8) and the boundary of the "forbidden zone" (Lindsley and Grover, 1980; Bohlen and Boettcher, 1981) to the one atmosphere relations in Figure 9a. Figures 10a–c compare the extrapolated 800°, 900°, and 1000°C isotherms in Figure 9d with the phase relations determined experimentally at 15 kbar for 810±10°, 905±10°, and 990±10°C (Table 3). For the most part the agreement is very good, although a number of the dissolving experiments at 810±10°C yield augite compositions that are slightly less calcic than the extrapolation would suggest. The extrapolated values are retained so that the thermometer will remain consistent with the results at higher temperatures and at lower pressures. The 1200°C isotherm in Figure 9d is mainly consistent with the 15-kbar data of Mori (1978); his results suggest that the pigeonite of the three-pyroxene triangle is slightly more calcic than is shown in Figure 9d, but they do not constrain it.

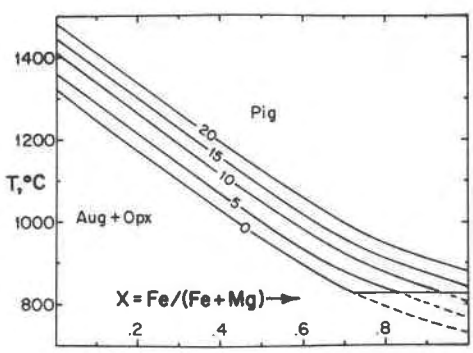

Fig. 8. The temperature of minimum stability for pure Ca–Mg–Fe pigeonite, relative to augite + orthopyroxene, as a function of X, for five pressures; curves are labelled in kbar. Note that the curves give only the X value of the *pigeonite* that coexists with augite and orthopyroxene; the augite and orthopyroxene are slightly more magnesian, as expressed by the widths of the three-pyroxene triangles in Figure 6. In contrast, the plot of Ross and Huebner (1979) shows the X value of the orthopyroxene that coexists with the pigeonite. The lines are dashed below 825°C to emphasize that Mn-poor pigeonites are not stable.

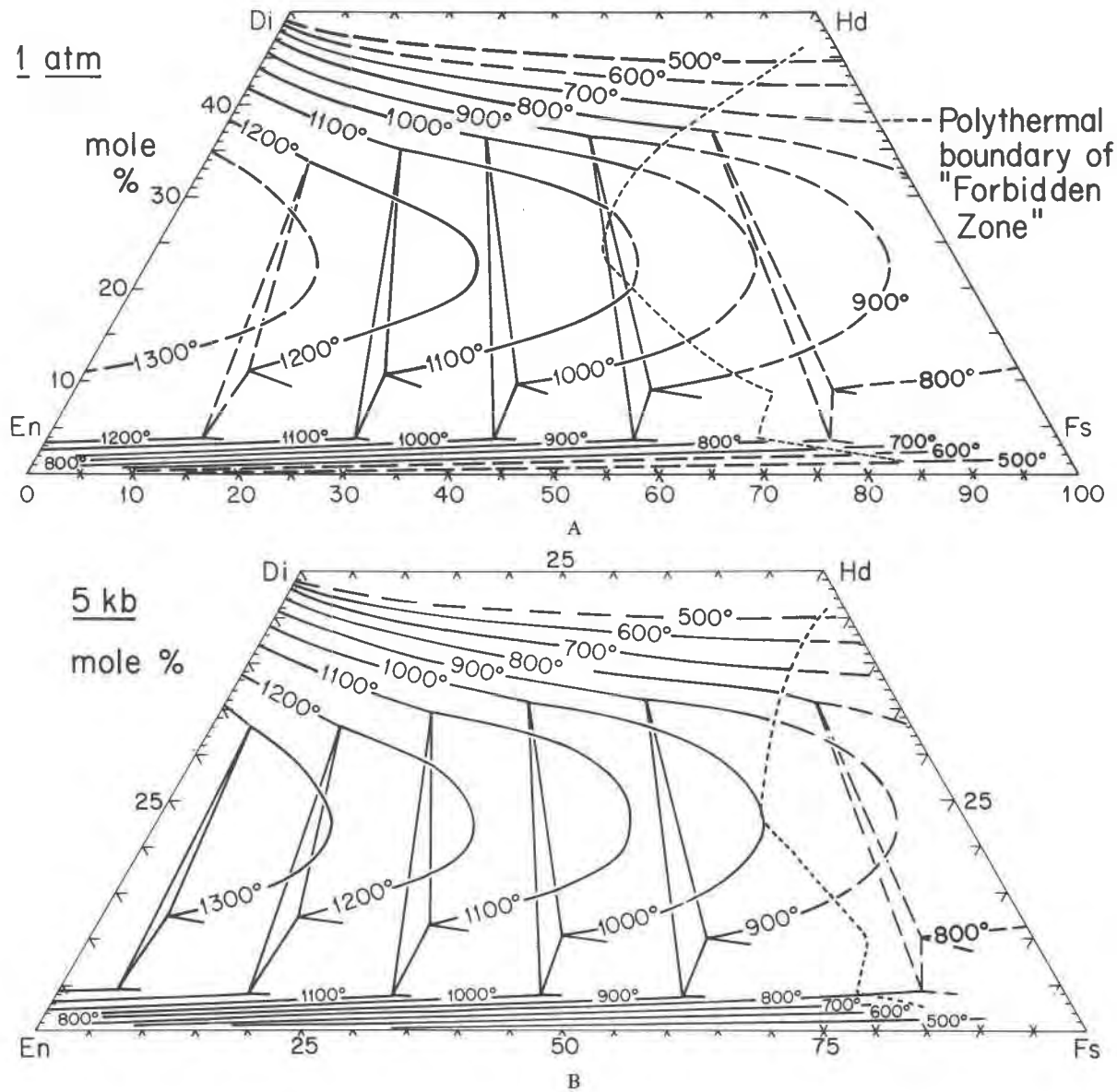

Fig. 9. Polythermal orthopyroxene + augite, orthopyroxene + augite + pigeonite, and pigeonite + augite relations, contoured at 100°C intervals for use in geothermometry. At various combinations of temperature and composition, the phase relations shown here may be metastable with respect to liquid, protopyroxene, ferrobustamite, olivine + silica, or combinations thereof. Compositions of most natural pyroxene pairs must be projected according to the scheme outlined in the text before they are plotted on these diagrams. Use of raw Wo-En-Fs data for all but very pure natural pyroxenes will yield incorrect temperatures and will not be tolerated. a. Relations at low pressure ($P < 2$ kbar). The 1300°C contour and those below 800°C are extrapolated from the Di–En and Hd–Fs diagrams (Figs. 4 and 5) so as to be compatible with the experimentally determined isotherms. b. Relations at 5 kbar. c. Relations at 10 kbar. d. Relations at 15 kbar. Figures 9b–d derived by extrapolation as described in the text. The short-dash curve in Figures 9a–c is the boundary of the "forbidden zone"; pyroxene relations to the right of that curve are metastable with respect to augite + olivine + silica.

Estimation of uncertainties

Lindsley and Andersen (1983) estimated that the placement of the isotherms in Figure 9a is accurate to approximately 20° to 30°C within the experimentally calibrated range, and similar uncertainties should apply to the 5, 10, and 15 kbar diagrams (Figs. 9b–d), although with larger uncertainties at 800°C and 15 kbar. Errors in composition probably introduce additional uncertainties of at least 20 to 30°C. Thus for pyroxenes having low contents of

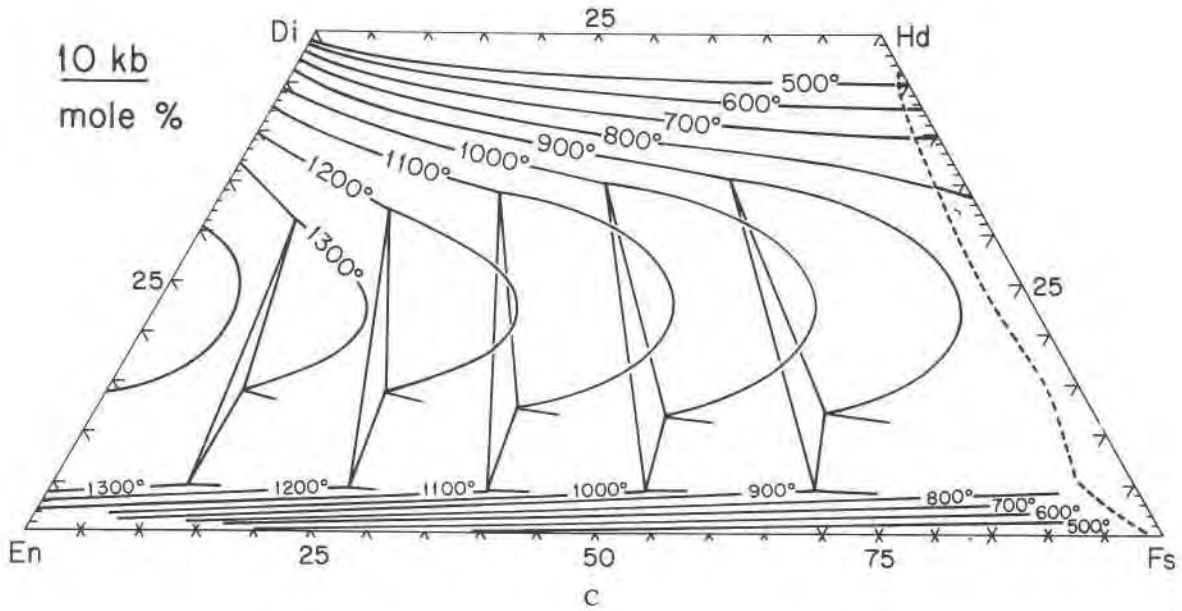

C

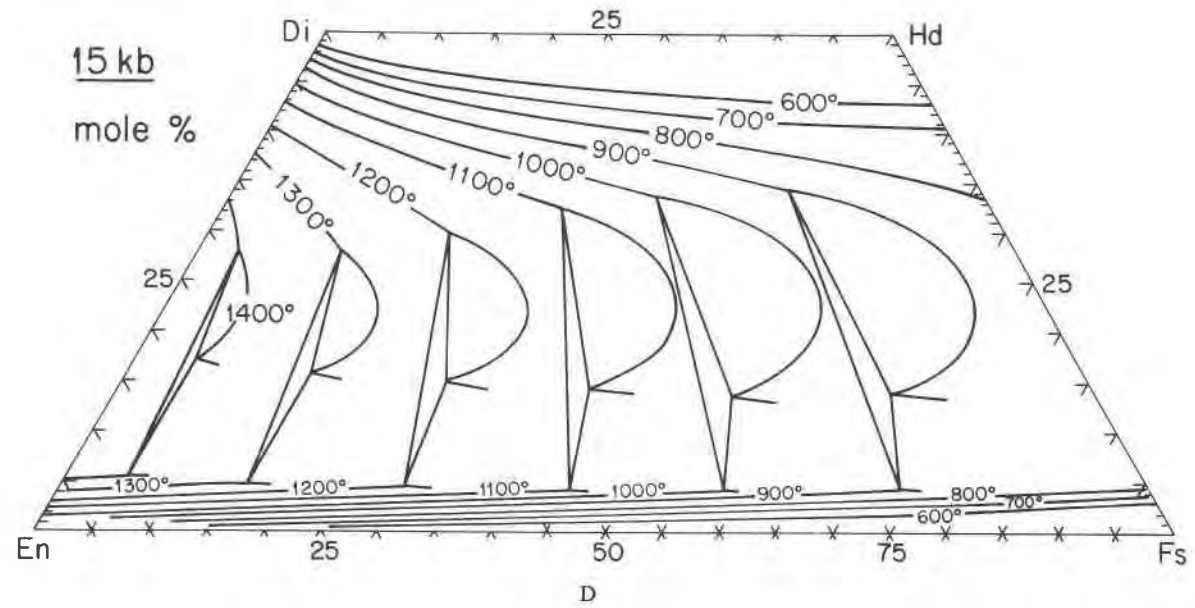

D

Fig. 9 (continued).

nonquadrilateral components, the thermometer probably is accurate to ±50°C. Correction for nonquadrilateral components (see below) will introduce additional uncertainties that will generally be proportional to the amounts of those components, although this effect is difficult to quantify. Lindsley and Andersen suggested that the uncertainty may increase by 5°C for each percentage point by which the proportion of nonquadrilateral components exceeds two mole percent.

Projection to the quadrilateral

Projection scheme

The projection scheme used (Lindsley and Andersen, 1983) is based on crystal-chemical considerations, experimental data where available, and a statistical study (Andersen, 1980 and unpublished data) of correlations among minor constituents in pyroxenes. Only an outline is

presented here; the reader is referred to Section 4 of Lindsley and Andersen for details. One calculates cations per 6 oxygens and assigns Si to the tetrahedral site, and Fe^{3+}, Ti, and Cr to the M1 site. Al is apportioned between the tetrahedral and M1 sites as outlined below. Ca and Na are restricted to the M2 site. Because the sole purpose of the projection scheme presented here is to obtain mole fractions of Wo, En, and Fs that most closely correspond to the bulk activities of those components, it is unnecessary to apportion Fe and Mg between the M1 and M2 sites.

Clinopyroxenes. Ferric iron is accepted from the chemical analysis where available. In that case tetrahedral and octahedral Al are then inferred from charge-balance considerations, through the relation (Papike *et al.*, 1974):

$$Al(VI) + Fe^{3+}(VI) + Cr(VI) + 2Ti^{4+}(VI) = Al(IV) + Na(M2)$$

and from the requirement that Al(IV) + Al(VI) = Al(Total). If only total Fe is available (as is the case for microprobe analyses), the sequence is different. Tetrahedral Al is taken as 2 − Si, with the remaining Al assigned to the M1 octahedral site. Fe^{3+} is then calculated from the charge-balance equation above. However, unless the analysis (especially for Si) is of superior quality, this step may seriously bias the results.

Now calculate the clinopyroxene components in the following sequence:

(1) Ac = $NaFe^{3+}Si_2O_6$ = Na or Fe^{3+}, whichever is smaller.
(2) Jd = Al(VI) or any remaining Na, whichever is smaller.
(3) FeCaTs = remaining Fe^{3+}.
(4) CrCaTs = Cr.
(5) AlCaTs = remaining Al(VI).
(6) For augite, "Ca" = Ca; for pigeonite, "Ca" = 2 − (Fe^{2+}+Mg). Finally, for clinopyroxenes, take Wo = ("Ca" + Ac − AlCaTs − FeCaTs − CrCaTs)/2, En = (1 − Wo) (1 − *X*), and Fs = (1 − Wo)(*X*), where *X* = $Fe^{2+}/(Fe^{2+}$ + Mg). Plot these Wo, En, and Fs values on Figure 9 to estimate the temperature.

Orthopyroxene. The projection scheme for orthopyroxene is slightly different: Al(IV) is taken as 2 − Si, and Al(VI) as Al(tot) − Al(IV). Ferric iron is then estimated from the charge-balance equation above. R^{3+} is taken as [Al(VI) + Cr + Fe^{3+}], and R^{2+} as [Mg(1 − *X*) + Fe^{2+}(*X*)]. Components are then calculated in the sequence:

(1) $NaR^{3+}Si_2O_6$ = Na or R^{3+}, whichever is smaller.
(2) $NaTiAlSiO_6$ = Ti or Al(IV) or any remaining Na, whichever is smallest.
(3) $R^{2+}TiAl_2O_6$ = the remaining Ti or [Al(IV)]/2, whichever is smaller.
(4) $R^{2+}R^{3+}AlSiO_6$ = the remaining R^{3+} or Al(IV); in a perfect analysis these would be equal.
(5) Ca, and the remaining Fe^{2+} and Mg, are then normalized to yield Wo + En + Fs = 1.

Note that the effect of this sequence is to maximize the content (and therefore the bulk activity) of Wo in the orthopyroxene. The resulting composition is then plotted on Figure 9 to yield the orthopyroxene temperature.

A program in BASIC to process chemical analyses of pyroxenes as outlined above will be supplied upon request. The program accepts data either as weight percent or as cations per six oxygens.

A word of caution. I should emphasize that this largely empirical projection scheme is an approximation only. Ordering of Fe and Mg between the M1 and M2 sites of pyroxenes may introduce additional complexities, especially at metamorphic temperatures. We also need more and better experimental data on the effects of additional

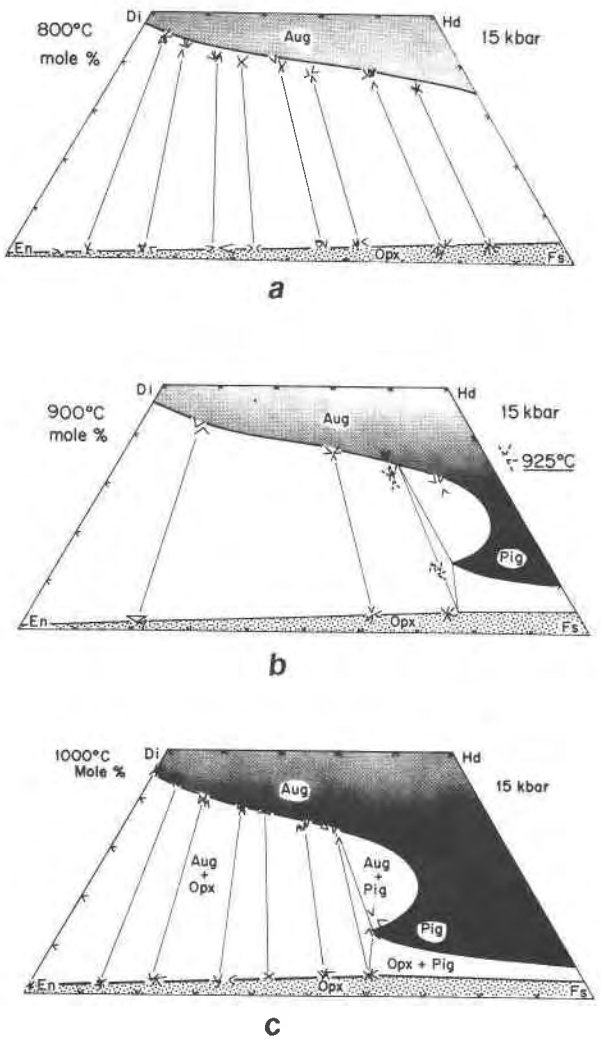

Fig. 10. Three 15-kbar isotherms from Figure 9d compared with experimental data obtained at 15 kbar (Table 3). a. The 800°C isotherm compared with data obtained at 810–815°C. b. The 900°C isotherm compared with data obtained mainly at 900–915°C. The dashed data symbols locate a three-pyroxene triangle for 925°C. c. The 1000°C isotherm compared with data obtained at 980–990°C.

components on the activities of quadrilateral components. For example, Suzanne Kay (pers. comm., 1982) has found that the apparent temperatures yielded by the thermometer increase with increasing alumina content: augites (from garnet granulites) with 8 wt.% Al_2O_3 yield temperatures in excess of 1000°C. Her results strongly suggest that the removal of the Tschermak's components (steps 3–5) from the effective Wo content of the augite is an overcorrection that results in an underestimation of the activity of Wo. Experimental evaluation of the effects of alumina on quadrilateral equilibria is urgently needed. In the meantime, use of the thermometer should be restricted to pyroxenes containing more than 90% Wo + En + Fs, and the user should bear in mind that the uncertainties increase with increasing amounts of nonquadrilateral components.

Applications of the two-pyroxene thermometer

Pyroxenes from lavas of known eruption temperatures

Probably the most appropriate samples for use of pyroxene thermometers are lavas with pyroxene phenocrysts. In at least some cases the phenocrysts may have crystallized in mutual equilibrium; eruption of the lava served to quench the samples and minimize any subsolidus re-equilibration. Groundmass pyroxenes, however, seem to have crystallized metastably in many cases and should be used with caution. Phenocryst (or microphenocryst) compositions have been determined for two lavas of known eruption temperature.

Mihara-yama. Ishii (1975) reported analyses of coexisting augite and orthopyroxene phenocrysts in a basalt from the 1950–1951 eruption of Mihara-yama Volcano, O-shima Island, Japan. The highest temperature observed during the eruption was 1125°C. Projected onto Figure 11, the compositions of the two augite phenocryst cores indicate 1100 and 1150°C; the orthopyroxene yields 1150°C for the temperature of crystallization. Especially in view of the possibility that the crystallization temperature of the phenocrysts may have been somewhat higher than that observed during the eruption, the correspondence is excellent. Ishii (1975) used this sample to define the 1125°C point on his three-pyroxene thermometer, apparently on the assumption that the groundmass pigeonite was in equilibrium with the phenocrysts. This assumption appears to be invalid; 1150°C would seem to be a better estimate for the temperature at which pigeonite would coexist with this augite and orthopyroxene.

Akita-komagatake. Aramaki and Katsura (1973) reported compositions of phenocrysts and microphenocrysts of pyroxenes in an andesite from the 1970–71 eruption of Akita-komagatake Volcano, northern Honshu. The highest observed temperature of the erupting lava was 1090°C; melting and crystallization experiments suggest an eruption temperature of 1100°C. The Ca contents of

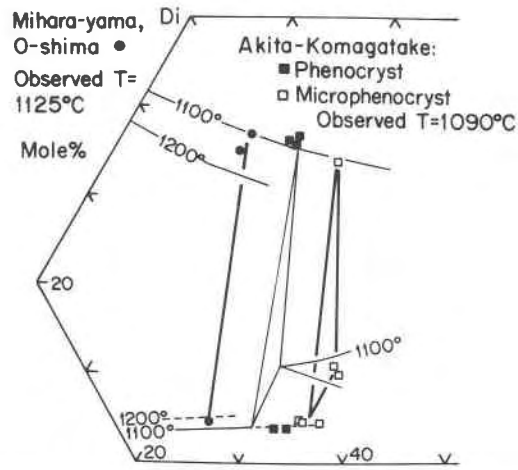

Fig. 11. Compositions of phenocryst augite and orthopyroxene (solid circles) from the 1950–1951 flow, Mihara-yama Volcano, O-shima, Japan (Ishii, 1975), projected onto part of the thermometer. The highest temperature observed during the eruption was 1125°C; the phenocrysts reflect this or a slightly higher, intratelluric temperature. Also shown are compositions of phenocrysts (solid squares) and microphenocrysts (open squares) from the 1970–71 flow, Akita-komagatake Volcano (Aramaki and Katsura, 1973). Eruption temperature of this flow was 1090–1100°C.

the augite and orthopyroxene phenocrysts (Fig. 11) are compatible with 1090°C, although the slope of the tie-line, which is more appropriate for an augite–*pigeonite* pair, raises some question as to whether the phenocrysts were in equilibrium. The microphenocrysts, presumed to have formed immediately prior to the eruption, form a classic three-pyroxene triangle. Both the augite and the orthopyroxene indicate a temperature at or just above 1100°C. The pigeonite microphenocrysts are also compatible with that temperature in view of the likelihood that nonquadrilateral components shift three-pyroxene triangles to more iron-rich compositions (Lindsley and Andersen, 1983, Section 3). Ishii (1975) used these samples to define the 1090°C point on his three-pyroxene thermometer; the Ross and Huebner pigeonite thermometer (1979) gives 1125°C.

Other three-pyroxene assemblages from lavas

The compositions of two reported three-pyroxene assemblages are plotted in Figure 12. The Funagata pyroxenes (Ishii, 1981) are all compatible with a temperature of 1200°C, in excellent agreement with the temperature of 1195°C as indicated by the minimum stability of pigeonite (Ross and Huebner, 1979). Like the three-microphenocryst assemblage from Akita-komagatake, this three-pyroxene triangle also indicates that the triangles for Mg-rich naturals may be displaced to slightly more Fe-rich compositions relative to those for the pure quadrilateral at a given temperature. Ishii (1981) estimated a temperature of 1155°C for Funagata. In contrast, the Weiselberg

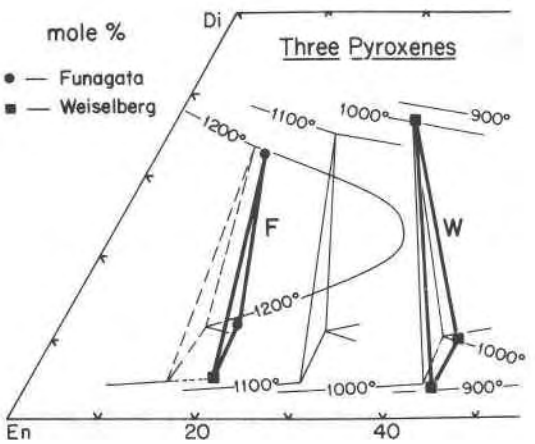

Fig. 12. Compositions of two reported three-pyroxene assemblages projected onto part of the thermometer. F (solid circles), Funagata (Ishii, 1981). W (solid squares), Weiselberg (Nakamura and Kushiro, 1970a).

samples (Nakamura and Kushiro, 1970a) plot very close to the pure three-pyroxene triangle for 1000°C, and the data are remarkably consistent with a crystallization temperature of 990°C. Note that for this more Fe-rich sample, the natural and pure Ca–Mg–Fe three-pyroxene triangles virtually coincide, confirming that determinations of the minimum stability of pigeonite in the quadrilateral are appropriate for more iron-rich natural samples. Ishii (1981) estimated a temperature of 1039°C for this assemblage, using his three-pyroxene thermometer (1975). The Ross–Huebner pigeonite thermometer (1979) suggests approximately 1090°C for the Weiselberg pyroxenes; Lindsley and Andersen (1983) suggest that temperatures from both these thermometers should be considered as upper limits rather than as actual crystallization temperatures for Fe-rich pyroxenes.

Other reported three-pyroxene assemblages. Several other three-pyroxene assemblages have been described in the literature [Hakone (Nakamura and Kushiro, 1970b; Ishii, 1981); Ashio (Kuno, 1969; Ishii, 1981)], but these appear not to have been in mutual equilibrium (Lindsley and Andersen, 1983).

Minimum stability of natural pigeonites—a thermometer

A distinct advantage of the present two-pyroxene (or three-pyroxene) thermometer over earlier thermometers based simply on the minimum stability of pigeonite (Ishii, 1975; Ross and Huebner, 1979; Podpora and Lindsley, 1979) is that independent estimates of temperature may be made from coexisting augite or orthopyroxene or both, as well as from the pigeonite. Nevertheless, there are times when a pigeonite thermometer can be very useful; when pigeonite is the only pyroxene to form, for example, such a thermometer gives a *minimum* value of the crystallization temperature. Figure 13 gives a best estimate for the minimum temperature of stability at low pressures of natural pigeonite relative to augite plus orthopyroxene. For Mg-rich pigeonites ($0.1 < X < 0.25$), the curve corresponds to that of Ross and Huebner (1979). Placement of the curve above that for pure Ca–Mg–Fe pigeonites in this region reflects the relative stabilization of augite + orthopyroxene by non-quadrilateral components and is consistent with the temperature deduced for the Funagata pyroxenes (discussed above). The curve is dashed in this region to emphasize that the actual temperature will depend on the amount of "others" in the pigeonite.

More Fe-rich pyroxenes tend to have fewer "others" components, and for them the determinations for the minimum stability of pigeonite in the pure system are appropriate. For example, Vocke (1981) experimentally determined the minimum stability for pigeonite (now inverted) from the metamorphosed Stillwater Iron Formation; her bracketed temperature of 825±20°C coincides with that of Podpora and Lindsley (1979) for pure quadrilateral pyroxenes having the same X value. The Weiselberg pyroxenes (cited above) likewise support this interpretation. Accordingly, the curve in Figure 13 uses the values for pure Ca–Mg–Fe pigeonites for $X > 0.5$. For $0.25 < X < 0.50$, the curve is sketched so as to connect the Ross–Huebner and Podpora–Lindsley curves; it passes through the temperature inferred for the Akita-komagatake three-pyroxene assemblage. Figure 13 should encompass the best features of the Ishii (1975), Ross and Huebner (1979), and Podpora and Lindsley (1979) pigeonite thermometers.

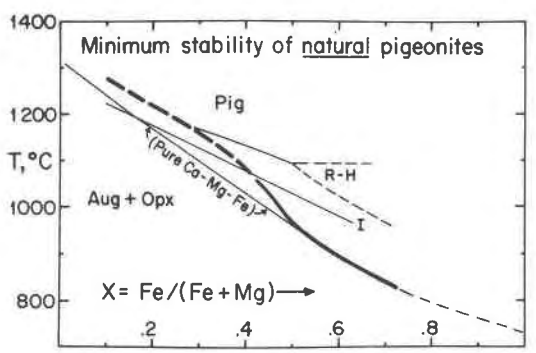

Fig. 13. Estimated plot (heavy curve) of the X value of natural pigeonites that coexist with augite + orthopyroxene at low pressures. Derivation is described in the text. R–H is Ross and Huebner (1979); I is Ishii (1975). The curve labelled (Pure Ca–Mg–Fe) is the 0-kbar curve from Figure 8, and was obtained from the data of Podpora and Lindsley (1979) and Lindsley and Andersen (1983). The heavy curve should give the minimum temperature at which a natural pigeonite of a given X value has crystallized. It should also yield the crystallization temperature of a pigeonite that coexisted with augite plus orthopyroxene, but that temperature should be checked against the augite and orthopyroxene temperatures obtained from Figure 9a.

Where pressure can be estimated independently, the apparent temperature from Figure 13 should be increased by 8.5°C per kbar (Lindsley and Grover, 1980; Lindsley and Andersen, 1983; Fig. 8 of this paper). Application of the pigeonite thermometer to inverted pigeonites in plutonic rocks obviously requires a reconstruction of the original composition—especially the X value—of the primary pigeonite.

Pigeonites are not stable at one atmosphere for X values >0.72. Lindsley and Grover (1980) showed that the effect of pressure in stabilizing pigeonite (relative to augite + olivine + quartz) to higher X values is just balanced by the simultaneous destabilization of pigeonite relative to Fe-rich augite + orthopyroxene. As a result, 825°C is the lowest temperature at which any Fe-rich quadrilateral pigeonite is stable (although approximately 10% $MnSiO_3$ component may further stabilize pigeonite down to 775°C; Bostwick, 1976). The X value of Mn-poor pigeonite coexisting with augite + orthopyroxene + olivine + quartz is a sensitive barometer: P(kbar) = $41.07(X_{pig} - 0.28)$, as revised from Lindsley and Grover (1980). Unfortunately this assemblage is rare.

Pyroxenes from plutonic rocks

Application of this or any two-pyroxene thermometer to plutonic rocks presents certain problems. Most plutonic pyroxenes are exsolved. The present compositions of the host pyroxene and exsolved lamellae should yield the temperature at which exsolution (on the scale resolved by the analytical technique used) effectively ceased. Recombination of host and lamellae into original compositions—which ideally yield magmatic or peak-metamorphic temperatures—may be tedious but should be straightforward. However, Hodges and Papike (1976), Bohlen and Essene (1978), and Lindsley and Andersen (1983) report a more subtle form of exsolution from some pyroxenes: granule exsolution, wherein the exsolved material migrates to form discrete grains at or near the edges of the original host. Failure to recognize these grains and to incorporate them into the reconstructed composition of the host may result in serious underestimation of the original temperature.

Skaergaard intrusion. Figure 2 shows the incongruity between the compositions of Mg-rich Skaergaard augites (as customarily plotted) and experimental data for pure quadrilateral pyroxenes. Projection of the Skaergaard augites by the scheme of Lindsley and Andersen (1983) removes some but not all of the problem: the apparent temperatures range from 1050°C for the most Mg-rich augite to 1100°C for the most Fe-rich augite that coexists with primary pigeonite. Nevertheless, the apparent increase of temperature with crystallization (increasing X) remains. Lindsley and Andersen (1983) present extensive textural, chemical, and experimental evidence that the Mg-rich augites from the Skaergaard have undergone significant amounts of granule exsolution, as have the

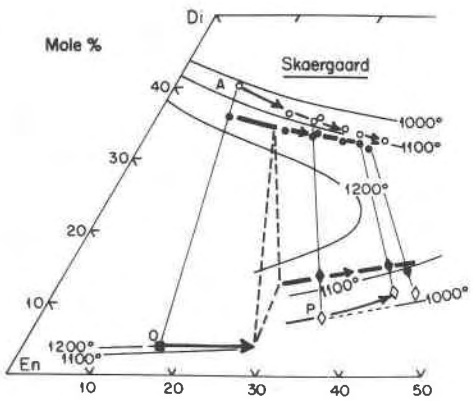

Fig. 14. A portion of the pyroxene quadrilateral showing selected isotherms (light curves) from the one-atmosphere thermometer (Fig. 9a). Also shown are the analyses of Mg-rich Skaergaard pyroxenes (Brown, 1957), *projected* by the method of Lindsley and Andersen (1983). The projected analyses and trends (open symbols and medium-weight lines) are more nearly compatible with the experimental data than are the raw Wo–En–Fs plots (see Fig. 2), but both the augite (A) and pigeonite (P) trends remain anomalous. The heavy trends and filled data symbols are *inferred* primary igneous trends and compositions for the augite and pigeonite; the differences are ascribed to near-solidus granule exsolution of augite from primary pigeonite and of pigeonite and/or orthopyroxene from primary augite (see Lindsley and Andersen, 1983).

pigeonites. Figure 14 presents inferred *primary* trends for Mg-rich Skaergaard pyroxenes, superimposed on a portion of the two-pyroxene thermometer. The discrepancies between these trends and the measured trends (as projected) are reflections of the probable degree of granule exsolution. Since the uncorrected augite trends for the Bushveld intrusion (Atkins, 1965) and other plutonic igneous bodies are similar to that for the Skaergaard (Brown, 1957), it seems likely that granule exsolution may be the rule for such bodies, and that application of the two-pyroxene thermometer to them will require painstaking reconstruction of primary pyroxene compositions. In many cases, unfortunately, unequivocal distinction between primary pyroxenes and exsolved granules may not be possible.

Application to granulites. Application of the thermometer to granulites has difficulties. For example, Bohlen and Essene (1979) concluded that none of the thermometers then in use gave consistent, meaningful temperatures for pyroxenes from Adirondack granulites. Sadly, that conclusion appears to hold for the present thermometer as applied to their data, which are microprobe analyses. With the present thermometer their clinopyroxenes show lower temperatures relative to the Wood–Banno thermometer but just as much scatter (from below 500° to 880°C), and there is no consistency with the temperatures inferred from two-feldspar and oxide thermometry. There is a tendency for alumina-rich clinopyroxenes to yield

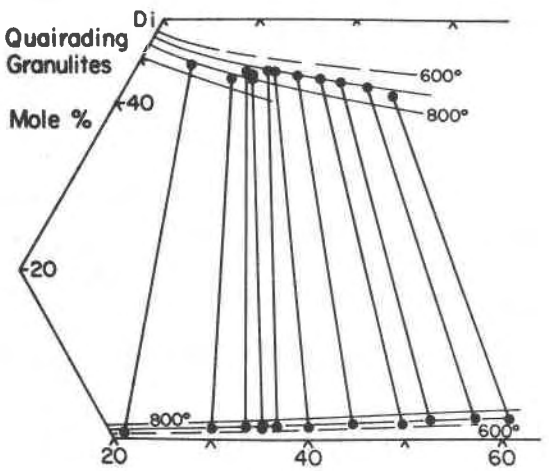

Fig. 15. Compositions of coexisting augites and orthopyroxenes from hornblende granulites, Quairading, Australia (Davidson, 1968), projected onto part of the thermometer.

higher temperatures, in agreement with the findings of Suzanne Kay (pers. comm.). The remaining scatter may reflect all or some of the following: incomplete resetting of igneous compositions, inadequate re-integration of exsolved material, or incorrect calculation of ferric iron. In contrast, their orthopyroxenes give temperatures ranging from 500 to 620°C, with the great majority above 550°C. Thus it is very tempting to conclude that the orthopyroxenes have been reset upon cooling from granulite grade, with blocking temperatures near 550°C.

Glassley and Sorensen (1980) also presented microprobe analyses of coexisting pyroxenes from a granulite terrane. The present thermometer applied to their orthopyroxenes gives very consistent temperatures clustered around 600°C. Either that represents a blocking temperature for the resetting of orthopyroxene compositions, or the thermometer is not suitably calibrated for very low-Ca orthopyroxenes. The clinopyroxenes indicate higher temperatures that unfortunately vary with the calculated ferric iron content. If all iron is presumed ferrous, the augites give temperatures from 580° to 710°C, with most between 630 and 700°C. Calculation of ferric iron as suggested by Lindsley and Andersen (1983) decreases the projected Wo content; the indicated temperatures range from 680 to 860°C, a much wider spread. It may be necessary to have independent determinations of ferric iron (perhaps by wet-chemical analysis or by Mössbauer spectroscopy) before the thermometer can be applied to these rocks.

Figure 15 shows compositions of coexisting augites and orthopyroxene from the hornblende granulites of Quairading, Australia (Davidson, 1968), as projected onto the two-pyroxene thermometer. At first glance, the Quairading pyroxenes seem ideal for application of the thermometer, for ferric iron was determined directly. The augites indicate temperatures ranging from 690 to 825°C (mean, 740±45°C) and the orthopyroxenes suggest 650 to 730°C (mean, 693±28°C). These temperatures should be increased by 16–23°C if the pressure of metamorphism is assumed to have been 5 kbar; the low-pressure temperatures are given here to facilitate comparison with other two-pyroxene thermometers that lack pressure corrections. The Mg-rich augites tend to yield slightly higher temperatures than the rest, although the difference may not be significant. Although the mean temperatures for augite and for orthopyroxene are not significantly different (the uncertainties are one standard deviation of the means), most of the orthopyroxenes tend to yield slightly lower temperatures than do the coexisting augites. It is unclear whether this difference reflects imprecision in the calibration of the thermometer (either in the placement of the isotherms or in the projection scheme) or whether the orthopyroxenes may have undergone some minor retrograde reaction that does not appear in the augites. It is also noteworthy that Davidson's orthopyroxene analyses consistently show about one-half mole percent more Wo than do the microprobe analyses cited above. Steven Bohlen (pers. comm., 1983) has pointed out that only a small amount of primary augite in the mineral separate could cause this difference, which corresponds to *ca.* 100°C on the orthopyroxene thermometer. Thus the better correspondence between orthopyroxene and clinopyroxene temperatures for Quairading may be fortuitous. Fortunately, minor contamination of the augite separate by primary orthopyroxene should have a much smaller effect on the augite temperatures.

It is noteworthy that despite the close spacing of the orthopyroxene isotherms of the thermometer, the temperatures indicated for suites of granulite orthopyroxenes are remarkably consistent. Presumably this is because the analytical errors in Ca are proportional to the amount of Ca present. Thus, if the dichotomy between wet-chemical and microprobe analyses can be resolved, the orthopyroxenes may eventually yield temperatures as good as those from the augites.

Ross and Huebner (1975) drew their 750°C isotherm to pass through the compositions of the Quairading augites. Kretz used these augites to define the projection path for metamorphic pyroxenes for his Ca thermometer (1982), and assumed that they formed at 730°C. Both of these assumed values are closely compatible with the temperatures yielded by the present thermometer. In contrast, other thermometers yield 863±35°C (Wood and Banno, 1973); 893±18°C (Wells, 1977); and 828±36°C (Saxena, 1976). These temperatures seem unrealistically high for hornblende granulites. For example, Bohlen and Essene (1977) used coexisting Fe–Ti oxides and coexisting feldspars to infer temperatures ranging from 650°C (hornblende granulites) to 790°C (garnet granulites) in the Adirondacks.

Summary and conclusions

Graphical thermometers based on equilibria of quadrilateral pyroxenes are presented for 1 atm and for 5, 10, and 15 kbar. The thermometers can be applied to augite–orthopyroxene, augite–pigeonite, and (to a limited extent) pigeonite–orthopyroxene pairs as well as to three-pyroxene assemblages. Each pyroxene of a pair or triplet yields an independent estimate of temperature, thereby permitting a check for consistency. The thermometer also gives a minimum temperature for the formation of single pyroxenes, since at or below the temperature of saturation a second pyroxene would have formed. The diagrams should be directly applicable to nearly pure (Wo + En + Fs > 98%) pyroxenes. The compositions of less pure pyroxenes should be projected onto the quadrilateral following the scheme of Lindsley and Andersen (1983). That correction scheme is largely empirical, because few experimental data of high quality are available regarding the effects of non-quadrilateral components on the compositions of coexisting pyroxenes. The projection must be refined on the basis of additional experiments; for example, the data of Kay (pers. comm., 1982) suggest that the scheme is not adequate for pyroxenes containing large amounts of alumina (8 wt.%). It is suggested that application be limited to pyroxenes in which Wo + En + Fs exceed 90%. Ultimately, the graphical thermometer will be replaced by a quadrilateral solution model fitted to the data, but the graphical approach should be useful in the interim.

Successful application of the two-pyroxene thermometer to slowly cooled rocks will usually require diligent reconstruction of primary pyroxene compositions on the basis of textural evidence. In particular, petrologists must be alert to the possibility of "granule exsolution"—the exsolution of low-Ca from high-Ca pyroxene (or vice versa) followed by the coalescence of the exsolved material into discrete grains, many of which may become external to the original parent grain. In many cases the resulting texture mimics that of primary crystallization and is therefore easy to overlook. Granule exsolution is most likely to occur at relatively high temperatures where diffusion rates are high; exsolution at lower temperatures generally yields the more familiar lamellar texture. Similar combinations of granule and lamellar exsolution are well known in some sulfides and (driven by oxidation) in Fe–Ti oxides. Although the reconstruction of original compositions may be tedious, there may be a bonus: in favorable cases it may be possible to determine not one but two or three temperatures—that of original crystallization, and those for the cessation of granule exsolution or of lamellar exsolution, or both.

At present it appears that mineral separation and wet-chemical analysis gives more satisfactory results for augites from granulite terranes than does re-integration of primary compositions from microprobe analyses. A direct measurement of ferric iron appears essential, since calculated Fe_2O_3 depends critically on the quality of the rest of the analysis, especially SiO_2. For orthopyroxenes from granulites, wet-chemical and microprobe methods each give very consistent results, but the former gives Wo contents that are higher by about 0.5 mole%; these yield "reasonable" granulite temperatures. The microprobe analyses, on the other hand, indicate temperatures mainly of 550 to 600°C, clearly too low for peak-granulite conditions. There are several possible explanations: (1) the wet-chemical analyses include but the microprobe analyses exclude small exsolved granules of Ca-rich pyroxene; temperatures indicated by the former are correct and reflect those of peak metamorphism; (2) the mineral separates of orthopyroxene were compromised by small amounts (1%) of *primary* (not exsolved) augite, and thus the temperatures they indicate are fortuitously good; (3) the microprobe analyses (with lamellae re-integrated where present) indicate true orthopyroxene compositions at granulite grade, and it is the orthopyroxene portion of the thermometer (or projection scheme) that is incorrect. Unfortunately, the present data do not permit discrimination among these possibilities.

Also presented is a revised thermometer based on the minimum stability of pigeonite.

Acknowledgments

I am grateful to many people who have contributed to this work over the years. Allan Turnock generously provided many of his pyroxenes used as starting materials; he and John Grover helped perform some of the experiments and provided many hours of stimulating discussions. Discussions with Steve Bohlen, Tim Grove, and Steve Huebner have also been most helpful. Steve Bohlen, Bob Dodd, and John Grover all improved the paper with their constructive comments. Selena Dixon, Hubert King, and Clara Podpora assisted with the experiments. It is a special pleasure to acknowledge the many contributions of David Andersen and Paula Davidson; they have played a major role in making this paper possible. In particular, Andersen helped develop the projection scheme and processed the analyses of hundreds of pairs of natural pyroxenes, and Davidson has contributed to the assessment of the experimental data and to the thermodynamic modelling of the pure pyroxenes. Work was supported by NASA grant # NGL-33-015-130 and by National Science Foundation, Earth Sciences Section, Grant EAR-8026250. My deep thanks go to them all.

References

Andersen, D. J. (1980) The "others" substitutional couples in terrestrial pyroxenes (abs). Geological Society of America, Abstracts with Programs, 12, 379.

Aramaki, S., and Katsura, T. (1973) Petrology and liquidus temperature of the magma of the 1970 eruption of Akita-komagatake Volcano, Northeastern Japan. Journal of the Japanese Association of Mineralogists, Petrologists, and Economic Geologists, 68, 101–124.

Atkins, F. B. (1965) The Pyroxenes of the Bushveld Igneous Complex, Transvaal. Ph.D. Thesis, University of Oxford.

Bohlen, S. R., and Boettcher, A. L. (1981) Experimental investi-

gations and geological applications of orthopyroxene geobarometry. American Mineralogist, 66, 951–964.

Bohlen, S. R., and Essene, E. J. (1977) Feldspar and oxide thermometry of granulites in the Adirondack Highlands. Contributions to Mineralogy and Petrology, 62, 153–169.

Bohlen, S. R., and Essene, E. J. (1978) Igneous pyroxenes from metamorphosed anorthosite massifs. Contributions to Mineralogy and Petrology, 65, 433–442.

Bohlen, S. R., and Essene, E. J. (1979) A critical evaluation of two-pyroxene thermometry in Adirondack granulites. Lithos, 12, 335–345.

Bostwick, T. R. (1976) The effect of Mn on the stability and phase relations of iron-rich pyroxenes. M.S. Thesis, State University of New York at Stony Brook.

Boyd, F. R. (1969) Electron-probe study of diopside inclusions from kimberlite. American Journal of Science, 267-A, (Schairer Volume), 50–69.

Boyd, F. R. (1973) A pyroxene geotherm. Geochimica et Cosmochimica Acta, 37, 2533–2546.

Brown, G. M. (1957) Pyroxenes from the early and middle stages of fractionation of the Skaergaard Intrusion, East Greenland. Mineralogical Magazine, 31, 511–543.

Davidson, L. R. (1968) Variations in ferrous iron-magnesium distribution coefficients of metamorphic pyroxenes from Quairading, Western Australia. Contributions to Mineralogy and Petrology, 19, 239–259.

Davidson, P. M., Grover, J. E. and Lindsley, D. H. (1982) $(Ca,Mg)_2Si_2O_6$ clinopyroxenes: a solution model based on non-convergent site-disorder. Contributions to Mineralogy and Petrology, 80, 88–102.

Davis, B. T. C., and Boyd, F. R., Jr. (1966) The join $Mg_2Si_2O_6$–$CaMgSi_2O_6$ and its application to pyroxenes from kimberlites. Journal of Geophysical Research, 71, 3567–3576.

Glassley, W. E., and Sorensen, K. (1980) Constant P_s–T amphibolite to granulite facies transition in Agto (West Greenland) metadolerites: implications and applications, Journal of Petrology, 21, 69–105.

Hodges, F. N., and Papike, J. J. (1976) DSDP site 334: Magmatic cumulates from Oceanic Layer 3. Journal of Geophysical Research, 81, 4135–4151.

Holland, T. J. B., Navrotsky, A. and Newton, R. C. (1979) Thermodynamic parameters of $CaMgSi_2O_6$–$Mg_2Si_2O_6$ pyroxenes based on regular solution and cooperative disordering models. Contributions to Mineralogy and Petrology, 69, 337–344.

Ishii, T. (1975) The relations between temperature and composition of pigeonite in some lavas and their application to geothermometry. Mineralogical Journal, 8, 48–57.

Ishii, T. (1981) Pyroxene geothermometry of basalts and an andesite from the Palau-Kyusho and west Mariana Ridges, Deep Sea Drilling Project Leg 59. Initial Reports of the Deep Sea Drilling Project, LIX, Naha, Okinawa to Apra, Guam, Sites 447-451, Feb.-March, 1978, 693–718.

Kretz, R. (1982) Transfer and exchange equilibria in a portion of the pyroxene quadrilateral as deduced from natural and experimental data. Geochimica et Cosmochimica Acta, 46, 411–422.

Kuno, H. (1969) Pigeonite-bearing andesite and associated dacite from Asio, Japan. American Journal of Science, 267A (Schairer Volume), 257–268.

Lindsley, D. H. (1980) Phase equilibria of Ca–Mg–Fe pyroxenes at pressures greater than 1 atm. Reviews in Mineralogy, 7, 289–307.

Lindsley, D. H. (1981) The formation of pigeonite on the join hedenbergite–ferrosilite at 11.5 and 15 kbar: Experiments and a solution model. American Mineralogist, 66, 1175–1182.

Lindsley, D. H., and Andersen, D. J. (1983) A Two-pyroxene thermometer. Proceedings of the Thirteenth Lunar and Planetary Science Conference, Part 2. Journal of Geophysical Research, 88, Supplement, A887–A906.

Lindsley, D. H., and Dixon, S. A. (1976) Diopside–enstatite equilibria at 850°–1400°C, 5–35 kbar. American Journal of Science, 276, 1285–1301.

Lindsley, D. H., and Grover, J. E. (1980) Fe-rich pigeonite: a geobarometer (abs). Geological Society of America, Abstracts with Programs, 12, 472.

Lindsley, D. H., and Munoz, J. L. (1969) Subsolidus relations along the join hedenbergite–ferrosilite. American Journal of Science, 267A (Schairer Volume), 295–324.

Lindsley, D. H., Grover, J. E. and Davidson, P. M. (1981) The thermodynamics of the $Mg_2Si_2O_6$–$CaMgSi_2O_6$ join: a review and an improved model. In R. C. Newton, A. Navrotsky and B. J. Wood, Eds., Advances in Physical Geochemistry, vol. 1, pp. 149–175. Springer, New York.

Lindsley, D. H., King, H. E. Jr., and Turnock, A. C. (1974) Composition of synthetic augite and hypersthene coexisting at 810°C: Application to pyroxenes from lunar highlands rocks. Geophysical Research Letters, 1, 134–136.

Mercier, J.-C. C. (1976) Single-pyroxene geothermometry and geobarometry. American Mineralogist, 61, 603–615.

Mori, T. (1978) Experimental study of pyroxene equilibria in the system CaO–MgO–FeO–SiO_2. Journal of Petrology, 19, 45–65.

Nakamura, Y., and Kushiro, I. (1970a) Equilibrium relations of hypersthene, pigeonite and augite in crystallizing magmas: microprobe study of a pigeonite andesite from Weiselberg, Germany. American Mineralogist, 55, 1999–2015.

Nakamura, Y., and Kushiro, I. (1970b) Compositional relations of coexisting orthopyroxene, pigeonite and augite in a tholeiitic andesite from Hakone volcano. Contributions to Mineralogy and Petrology, 26, 265–275.

Papike, J. J., Cameron, K. L. and Baldwin, K. (1974) Amphiboles and pyroxenes: Characterization of OTHER than quadrilateral components and estimates of ferric iron from microprobe data (abstract). Geological Society of America, Abstracts with Programs, 6, 1053–1054.

Podpora, C., and Lindsley, D. H. (1979) Fe-rich pigeonites: minimum temperatures of stability in the Ca–Mg–Fe quadrilateral (abstract). EOS, (Transactions of the American Geophysical Union), 60, 420–421.

Ross, M., and Huebner, J. S. (1975) A pyroxene thermometer based on temperature–composition relationships of naturally occurring orthopyroxene, pigeonite, and augite (extended abstract). International Conference on Geothermometry and Geobarometry, Penn. State Univ., Oct. 5–10, 1975.

Ross, M., and Huebner, J. S. (1979) Temperature–composition relationships between naturally occurring augite, pigeonite, and orthopyroxene at one bar pressure. American Mineralogist, 64, 1133–1155.

Saxena, S. K. (1976) Two-pyroxene geothermometer: A model with an approximate solution. American Mineralogist, 61, 643–652.

Saxena, S. K., and Nehru, C. E. (1975) Enstatite–diopside solvus and geothermometry. Contributions to Mineralogy and Petrology, 49, 259–267.

Turnock, A. C., and Lindsley, D. H. (1981) Experimental

determination of pyroxene solvi for P ≤ 1 kb, 900 and 1000°C. Canadian Mineralogist, 19, 255–267.

Turnock, A. C., Lindsley, D. H. and Grover, J. E. (1973) Synthesis and unit-cell parameters of Ca–Mg–Fe pyroxenes. American Mineralogist, 58, 50–59.

Vocke, C. M. (1981) T-fO_2 conditions of the metamorphism of the Stillwater Iron Formation, Montana. M.S. Thesis, State University of New York, Stony Brook.

Wells, P. R. A. (1977) Pyroxene thermometry in simple and complex systems. Contributions to Mineralogy and Petrology, 62, 129–139.

Wood, B., and Banno, S. (1973) Garnet–orthopyroxene and orthopyroxene–clinopyroxene relationships in simple and complex systems. Contributions to Mineralogy and Petrology, 42, 109–124.

Manuscript received, January 17, 1983;
accepted for publication, January 24, 1983.